Journal Pre-proofs

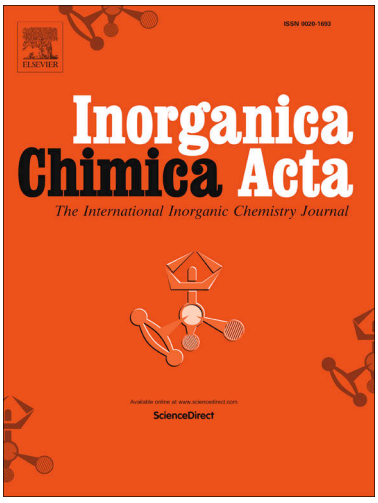

Research paper

Development of tris-cyclometalated iridium complexes for cellular imaging through structural modification

Sureemas Meksawangwong, Bhavini Gohil, Wikorn Punyain, Robert Pal, Filip Kielar

PII: S0020-1693(20)30123-7
DOI: https://doi.org/10.1016/j.ica.2020.119609
Reference: ICA 119609

To appear in: *Inorganica Chimica Acta*

Received Date: 23 January 2020
Revised Date: 18 March 2020
Accepted Date: 19 March 2020

Please cite this article as: S. Meksawangwong, B. Gohil, W. Punyain, R. Pal, F. Kielar, Development of tris-cyclometalated iridium complexes for cellular imaging through structural modification, *Inorganica Chimica Acta* (2020), doi: https://doi.org/10.1016/j.ica.2020.119609

Development of tris-cyclometalated iridium complexes for cellular imaging through structural modification

Sureemas Meksawangwong[a], Bhavini Gohil[b], Wikorn Punyain[a], Robert Pal[b] Filip Kielar*[a]

a) Department of Chemistry and Center of Excellence in Biomaterials, Faculty of Science, Naresuan University, Phitsanulok 65000, Thailand
b) Department of Chemistry, Durham University, South Road, Durham, DH1 3LE, UK

Abstract

Herein we report the synthesis and investigation of two novel tris-cyclometalated iridium complexes derived from [Ir(ppy)$_3$] and bearing an aminoalkyl substituent on one of the 2-phenylpyridine ligands. These complexes differ in the number of the alkyl substituents of the aminoalkyl group. Specifically, the complexes reported herein contain one (**1**) and two (**2**) 2-hydroxy ethyl groups on the nitrogen atom. Both complexes retain the good photophysical properties reported for earlier versions of this group of tris-cyclometalated iridium complexes. However, the differences in the substitution results in changes in the responsive photoluminescence behavior in aqueous solutions. Live cell microscopy experiments revealed that complexes can localize in NIH-3T3 cells. Finally, it has been observed that the complex containing two 2-hydroxy ethyl groups is less cytotoxic than the it's mono-substituted counterpart.

Keywords

Iridium; Cellular Imaging; Photoluminescence

Corresponding Author:
Filip Kielar
Department of Chemistry
Naresuan University
Phitsanulok
65000
Thailand
filipkielar@nu.ac.th

Introduction

Cyclometalated iridium complexes have received significant amount of interest in recent years.[1-3] This is attributed to their rich photochemical properties, which results in their utility in areas such as cellular imaging, Organic Light Emitting Devices (OLEDs), potoredox catalysis, and others.[4-9] Luminescence lifetimes reaching the microsecond regime, large Stokes' shifts, and ease of spectral tuning of emission are the key favorable properties of these compounds. These desirable bio-physical properties result from the interplay of the iridium ion and its ligands. The large (5d) iridium ion carrying a relatively high charge (+3) together with the strong sigma donating character of the cyclometalating ligands ensure large ligand field.[3] This results in lack of involvement of deactivating metal centered (MC) transitions in the photophysical properties of the complexes and in turn results in photophysics based around ligand centered, metal to ligand charge transfer (MLCT) centered, and other charge transfer transitions.[10] Furthermore, the high spin-orbit coupling constant of the iridium center relaxes the forbidden nature of transitions between singlet and triplet states.[11-13] This results in efficient intersystem crossing and emission that is phosphorescent in nature. Thus, the luminescence lifetimes of cyclometalated iridium complexes can reach the microsecond regime, which is significantly longer than for organic fluorophores yet much shorter than observed for phosphorescence from purely organic systems. Finally, the charge transfer nature of the phtophysical transitions results in localization of the HOMO and LUMO orbitals on different parts of the complexes. This leads to relatively facile tuning of the emission bands as independent modulation of the HOMO or LUMO orbitals is possible.[14-15]

The relatively long luminescence lifetimes and large Stokes' shifts observed in cyclometalated iridium complexes are useful for bio-imaging purposes as they enable more facile separation of excitation and emission as well as separation of light emitted from the probe of the background auto-fluorescence.[2, 16-17]

Bis-cyclometalated iridium complexes is identified as the dominant structural class utilized in cellular imaging. This is mainly due to the facile synthesis of these complexes as well as their ability to carry a single positive charge which is assumed to be beneficial for cellular uptake during imaging experiment.[13] The tris-cyclometalated iridium complexes that are frequently utilized in other applictations are considered to be superior to the bis-cyclometalated with respect to their photophysical properties but utilized to a much smaller extent. It appears that they are, in general, less efficiently internalized by cells due to being charge neutral.[18-20]

Our research group has recently published a report on two aminoalkyl substituted tris-cyclometalated iridium complexes derived from the archetypal complex [Ir(ppy)$_3$] (**Figure 1**), which carry an aminoalkyl group on one of the 2-phenylpyridine ligands.[21] The previously published complexes contained butyl and dodecyl chains on the amino group. These complexes have shown interesting photophysial properties, including a ratiometric response of their emission to pH, which was structure dependent. The possibility to utilize these complexes in cellular imaging has also been demonstrated. Derived form these promising results, we decided to synthesize further analogues of these compounds, which we report herein. The newly synthesized complexes bearing one and two 2-hydroxyethyl substituents on the amino group. The first one was synthesized as a direct analogue of

the previously reported complexes containing simple alkyl groups while the latter was synthesized with reduced cytotoxicities in mind as it was observed for complexes where the secondary amino group is transformed into its tertiary amino analogue or a quarternary ammonium group.[21-22]

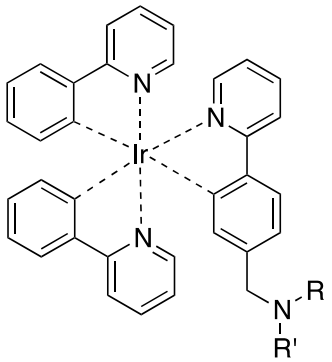

Previous report
R = H, R' = C_4H_9
R = H, R' = $C_{12}H_{25}$

This report
R = H R' = CH_2CH_2OH, [Ir(ppy)$_2$ppy-N-OH], (**1**)
R, R' = CH_2CH_2OH, [Ir(ppy)$_2$ppy-N-(OH)$_2$], (**2**)

Figure 1. Structures of tris-cyclometalted aminoalkyl iridium complexes reported by our group.

Experimental

General comments

Unless otherwise stated, all commercial reagents were used as received. Silver trifluoromethanesulfonate, ethanolamine, diethanolamine, and sodium borohydride were purchased from Sigma Aldrich. Sodium cyanoborohydride, 2-phenylpyridine (ppy), 2-ethoxyethanol, and silicagel were purchased from Merck. Butylamine, methyl iodide, and iridium(III)chloride trihydrate were purchased from Fisher. Dichlromethane, methanol, and triethyl amine were purchased from Carlo Erba. Sodium bicarbonate, anhydrous sodium sulphate, and trisodium phosphate were purchased from Univar. Acetonitrile and dimethyl sulfoxide were purchased from RCI. The precursor complex [Ir(ppy)$_2$(fppy)] was synthesized as previously reported.[21] ^{1}H and ^{13}C NMR spectra were recorded on a Bruker Avance 400 MHz instrument operating at 400 MHz and 100 MHz for proton and carbon, respectively. Mass spectra were recorded with an Agilent technologies UHD Accurate-Mass Q-TOF LC-MS instrument model 6540. UV-Visible spectra were recorded using Analytik Jena 210plus diode array spectrophotometer. Steady state emission spectra were recorded using Fluoromax-4 spectrofluorometer from Yvon Horiba. Phoshorescence lifetime measurements were performed on the DeltaFlex^{TM} instrument equipped with a UV LED (λ_{ex} = 372 nm). Cell viability was determined using the Chemometec NucleoCounter-3000 cell analyzer.

*Synthesis of fac-[Ir(ppy)$_2$ppy-N-OH], (**1**)*

[Ir(ppy)$_2$fppy] (0.22 mmol, 150 mg), ethanolamine (0.44 mmol, 27 µL), and triethylamine (0.22 mmol, 31 µL) were suspended in methanol:dichloromethane 1:1 mixture (10:10 mL).

The mixture was heated at reflux under nitrogen for 10 h. The solution was left to cool to room temperature, and $NaBH_4$ (0.44 mmol, 16.6 mg) was added. The reaction mixture was stirred at room temperature for 20 h. The solvent was removed under vacuum. The residue was dissolved in dichloromethane, dried over anhydrous sodium sulphate, and filtered. The solvent was completely removed under reduced pressure and the residue was dissolved in dichloromethane and purified by column chromatography on silica using gradient of methanol (up to 15%) in dichloromethane as the eluent. The pure product was isolated as an orange solid (0.10 mmol, 73.0 mg, 45 %). ^{1}H NMR (400 MHz, CD_3OD, δ)) 2.81 (*m*, 2H), 3.62 (*m*, 2H), 3.78 (*m*, 2H), 6.65-6.76 (*m*, 4H), 6.83 (*m*, 3H), 6.89-6.98 (*m*, 4H), 7.52 (*m*, 2H), 7.57 (*m*, 1H), 7.60-7.71 (*m*, 5H), 7.76 (*d*, *J* = 8.0 Hz, 1H), 7.95 (*d*, *J* = 8.0 Hz, 1H), 8.00 (*m*, 2H).^{13}C NMR (100 MHz, CD_3OD, δ) 49.92, 52.63, 58.24, 119.99, 120.35, 121.01, 120.04, 121.75, 123.26, 123.32, 123.80, 125.15, 125.18, 125.56, 130.34, 130.48, 133.92, 137.70, 137.74, 173.78, 173.85, 138.01, 139.20, 145.37, 145.38, 146.78, 148.27, 148.39, 148.52, 161.56, 161.93, 163.70, 166.97, 167.81. HRMS (ES^+) calcd. for $C_{36}H_{32}IrN_4O$ (729.2205); found (729.2228) $[M+H]^+$.

*Synthesis of fac-[Ir(ppy)$_2$ppy-N-(OH)$_2$], (**2**)*

[Ir(ppy)$_2$fppy] (0.078 mmol, 53 mg), diethanolamine (0.12 mmol, 12 µL), and triethylamine (0.078 mmol, 11 µL) were suspended in methanol:dichloromethane 1:1 mixture (7:7 mL). The mixture was heated at reflux under nitrogen for 10 h. The solution was left to cool to room temperature, and $NaBH_4$ (0.078 mmol, 3 mg) was added. The reaction mixture was stirred at room temperature for 20 h. The solvent was removed under vacuum. The residue was dissolved in dichloromethane, dried over anhydrous sodium sulphate, and filtered. The solvent was completely removed under reduced pressure and the residue was dissolved in dichloromethane and purified by column chromatography on silica using gradient of methanol (up to 15%) in dichloromethane as the eluent. The pure product was isolated as an orange solid (0.040 mmol, 30.8 mg, 51 %). ^{1}H NMR (400 MHz, CD_3OD, δ)) 3.08 (*m*, 4H), 3.69 (*m*, 4H), 4.09 (*s*, 2H), 6.63 (*dd*, *J* = 7.6 Hz, *J* = 1.2 Hz, 1H), 6.68 (*dd*, *J* = 7.2 Hz, *J* = 1.2 Hz, 1H), 6.73 (*m*, 2H), 6.78 (*d*, *J* = 4.0 Hz, 1H), 6.85 (*m*, 2H), 6.97 (*m*, 3H), 7.04 (*m*, 1H), 7.57 (*m*, 1H), 7.60 (*m*, 1H), 7.63 (*m*, 1H), 7.71 (*m*, 5H), 7.80 (*d*, *J* = 8.0 Hz, 1H), 8.01 (*m*, 2H), 8.06 (*d*, *J* = 8.0 Hz, 1H).^{13}C NMR (100 MHz, CD_3OD, δ) 55.50, 56.55, 58.43, 119.99, 120.07, 120.60, 121.08, 121.15, 123.32, 123.45, 123.57, 124.18, 125.20, 125.25, 125.52, 130.43, 130.62, 137.67, 137.77, 137.86, 137.92, 137.93, 140.92, 145.36, 148.38, 145.45, 148.73, 161.35, 161.81, 163.95, 166.66, 167.73, 167.81. HRMS (ES^+) calcd. for $C_{38}H_{36}IrN_4O_2$ (773.2468); found (773.2470) $[M+H]^+$.

Photochemical measurements

Unless otherwise stated, stock solutions of iridium complexes (0.5 mM) were prepared in DMSO. They were then diluted to their desired concentration (typically 10 µM) with the appropriate solvent. The measurements were performed in quartz cuvettes of 1 cm path length. Degassing of the samples for lifetime measurements have been achieved by bubbling nitrogen gas through them for 10 minutes in order to eliminate the presence of oxygen.

Luminescence quantum yields were determined using *fac*-[Ir(ppy)$_3$] in degassed dichloromethane solution as the standard, for which Φ_{lum} = 0.89.[23] The solutions for this measurement were degassed by four cycles of freeze-pump-thaw.

Luminescence lifetimes of the complexes were measured by time-correlated-single-photon-counting (TCSPC) using a laser diode (372 nm) as the excitation source. The estimated error in the lifetimes is 10%.

DFT Calculations

Calculations were carried out with the Gaussian09 software package at the DFT level, using the hybrid functional B3LYP and the double-zeta basis set LANL2DZ.[24] The calculations were carried out for a vacuum environment as well dichloromethane (ε = 8.93) using the polarizable continuum model. The molecular orbitals were visualized using the Gabeit program package.[25]

Cell Culture

A detailed investigation of the cellular behaviour of each complex was conducted using mouse skin fibroblasts (NIH-3T3) and human prostate adenocarcinoma (PC3) cell lines using fluorescence and laser scanning confocal microscopy. Cells were maintained in exponential growth as monolayers in F-12/DMEM (Dulbecco's Modified Eagle Medium) 1:1 that was supplemented with 10% foetal bovine serum (FBS). Cells were grown in 75 cm^2 plastic culture flasks, with no prior surface treatment. Cultures were incubated at 37 °C, 20% average humidity and 5% (v/v) CO_2. Cells were harvested by treatment with 0.25% (v/v) trypsin solution for 5 min at 37 ºC. Cell suspensions were pelleted by centrifugation at 1000 rpm for 3 min, and were re-suspended by repeated aspiration with a sterile plastic pipette. Cells destined for Microscopy experiments were seeded in 12-well plates on 13mm 0.170mm thick standard glass cover-slips or un-treated iBibi 100 uL live cell channels and allowed to grow to 40% – 60% confluence, at 37 ºC in 5% CO_2. At this stage, the medium was replaced and cells were treated with complexes and co-stains as appropriate. For imaging DMEM media (10% FBS) lacking phenol red (live cell media) was used from this point onwards. Following incubation, the cover-slips were washed with live cell media, mounted on slides and the edges sealed with colourless, quick-dry nail varnish to prevent drying out of the sample.

Cell toxicity measurements were run using a ChemoMetec A/S NucleoCounter3000-Flexicyte instrument with Via1-cassette cell viability cartridge (using the cell stain Acridine Orange for cell detection, and the nucleic acid stain DAPI for detecting non-viable cells). The experiments were done in triplicate. In cellular uptake studies cells were seeded in 6-well plates and allowed to grow to 80% – 100% confluence, at 37 ºC in 5% CO_2. At this stage, the medium was replaced with media containing targeted complexes as detailed above and total cellular Iridium was determined using ICP-MS, inductively coupled plasma mass spectrometry by Dr. C. Ottley in the Department of Earth Sciences at Durham University.

Steady state fluorescence microscopy

Steady state fluorescence images were recorded using a PhMoNa[26] enhanced Leica SP5 II LSCM confocal microscope equipped with a HCX PL APO 63x/1.40 NA LambdaBlue Oil immersion objective. Data were collected using 2.5x digital magnification at 400 Hz/line scan speed (4 line average, bidirectional scanning) at 355 nm (3^{rd} harmonic NdYAG laser) with 3 mW laser power (80 nJ/voxel). In order to achieve excitation with maximal probe emission, the microscope was equipped with a triple channel imaging

detector, comprising a conventional PMT systems and two HyD hybrid avalanche photodiode detector. The latter part of the detection system, when operated in the BrightRed mode, is capable of improving imaging sensitivity by 25%, reducing signal to noise by a factor of 5. Frame size was determined at 2048 x 2048 pixel, with 0.6 airy disc unit determining the applied pinhole diameter rendering on voxel to be corresponding to 24.02 x 24.02 nm (frame size 49.16 x 49.16 µm) with a section thickness of 380 nm. A HeNe or Ar ion laser was used when commercially available organelle-specific stains (e.g. MitoTrackerRed^{TM}) were used to corroborate cellular compartmentalization. Spectral imaging on this Leica system is possible with the *xyλ*-scan function, using the smallest allowed spectral band-pass (5nm) and step-size (3nm) settings. However, much improved spectral imaging in cells was achieved using a custom built microscope (modified Zeiss Axiovert 200M), using a Zeiss APOCHROMAT 63x/1.40 NA objective combined with a low voltage (5 V) 365 nm pulsed UV LED focused, collimated excitation source (1.2W). For rapid spectral acquisition the microscope was equipped at the X1 port with a Peltier cooled 2D-CCD detector (Ocean Optics, MayaPro2000) used in an inverse 100 Hz time gated sequence. The spectrum was recorded from 400-800 nm with a resolution of 0.24 nm and the final spectrum was acquired using an averaged 10,000 scan duty cycle. Probe lifetimes were measured on the same microscope platform using a novel cooled PMT detector (Hamamatsu H7155) interchangeable on the X1 port, with the application of pre-selected interference filters matched to as selected in live cell LSCM experiments. Both the control and detection algorithm were written in LabView2013, where probe lifetime was determined by using a single exponential fitting algorithm to the monitored signal intensity decay.

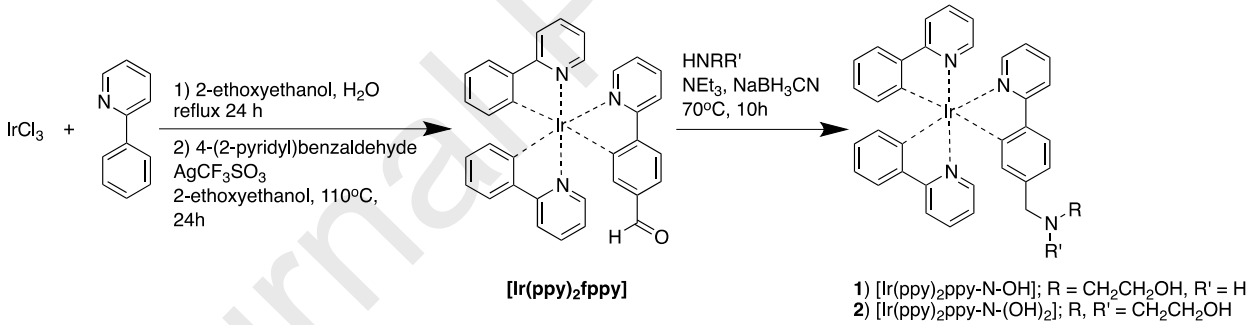

Scheme 1. Synthesis of complexes **1** and **2**

Results and discussion

Synthesis

The complexes have been synthesized using slight modifications of the procedures from our previous report. In short, the complexes were prepared in three steps. The first step is the synthesis of a chloride bridged iridium dimer from iridium chloride and 2-phenyl pyridine using the Nonoyama reaction. This was followed by the transformation of the dimer using 4-(pyridine-2-yl)benzaldehyde into a monomeric complex [Ir(ppy)$_2$fppy]. Finally, the novel aminoalkyl iridium complexes were synthesized in a reductive amination reaction with ethanolamine and diethanolamine to give complexes **1** and **2**, respectively (**Scheme 1**). The complexes were characterized by ^{1}H-NMR, ^{13}C-NMR, and HRMS.

Photophysical properties

The UV-vis absorption and PL emission spectra of complexes **1** and **2** recorded in dichloromethane exhibit the same features. The absorption spectra can be divided into three key regions. Firstly, the strong absorption observed below 320 nm and centered around 280 nm can be assigned to allowed π to $\pi*$ transitions in the ligands (**Figure 2**). The weaker absorption band centered at 390 nm corresponds to singlet metal to ligand charge-transfer transitions (^{1}MLCT) while the weak tail extending beyond 450 nm originates from forbidden triplet metal to ligand charge-transfer transition (^{3}MLCT). The steady state emission spectra of both complexes in dichlomethane exhibit a single peak with a maximum at 513 nm (**Figure 2**). The photophysical properties are further summarized in **Table 1**.

Table 1. Photophysical properties of complexes **1** and **2**

	1	**2**
Absorption (λ_{max}/nm)[a]	283, 376	283, 380
Emission (λ_{max}/nm)[a]	513	513
Quantum Yield (Φ_{lum})[a]	0.91	0.98
Lifetime (ns)[a]	1422 (51)	1301 (44)
Lifetime (ns)[c]	322	176

a) dichloromethane, b) dimethylsulfoxide, c) tetrahydrofuran

The quantum yields observed for both complexes are on the order of 40% and are similar to the parent complex and our previously reported structures. Same conclusion can be drawn for the luminescence lifetime. Complex **1** exhibits lifetimes of 41 ns and 1.42 μs in aerated and degassed dichloromethane solutions, respectively, while complex **2** exhibits lifetimes of 44 ns and 1.30 μs under these conditions. The similarity of the photophysical properties of complexes **1** and **2** with each other and with our previously reported compounds were further demonstrated by the results of Density Functional Theory (DFT) calculations carried out using the polarizable continuum model for dichloromethane solution at the B3LYP/LANL2DZ level of theory. The results of this calculation are shown in **Figure 3**, which demonstrates that the HOMO orbital for both complexes is mainly located on the iridium atom while the LUMO orbital is predominantly located on the cyclometalating ligand carrying the aminoalkyl substituent. This is consistent with the expected MLCT nature of the electronic transitions in this type of cyclometalated iridium complexes. In addition, the calculated energy difference between these orbitals is 3.50 eV, which is consistent with the observed absorption spectrum. Furthermore TD-DFT calculations have been carried out to model the UV-Vis spectra of complexes **1** and **2**. Comparison of the experimental and calculated spectra can be seen in **SI Figure 7**, which shows a good match between the observed and simulated data.

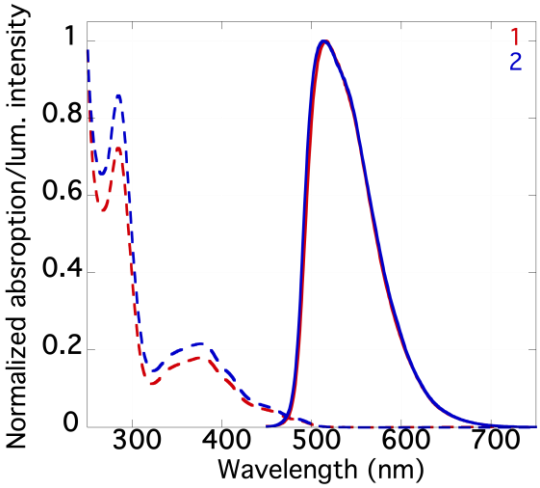

Figure 2. Normalized absorption (dashed) and emission (full) spectra of complexes **1** (red) and **2** (blue) (10 μM) recorded in dichloromethane (λ_{ex} = 390 nm)

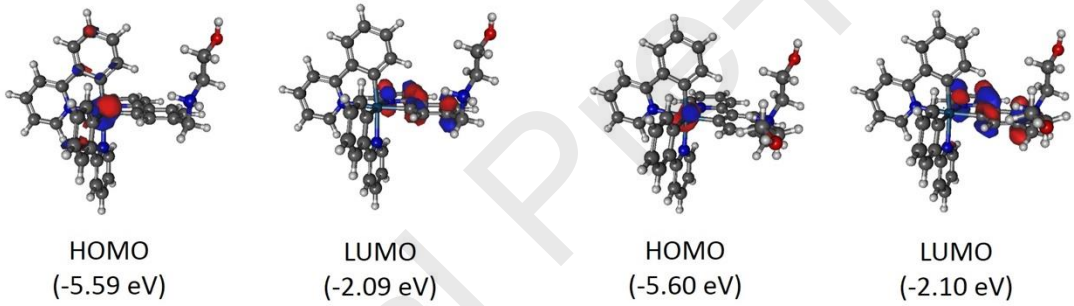

Figure 3. The HOMO and LUMO orbitals of complexes **1** (left) and **2** (right) calculated in dichloromethane.

While the photophysical properties of complexes **1** and **2** are very similar in dichloromethane, they exhibit significant differences in aqueous media. Complex **1** shows a single emission peak with a maximum around 530 nm, complex **2** displays a structured emission spectrum with a maximum at 580 nm and a shoulder around 520 nm (**Figure 4**). The emission spectrum of this class of complexes depends on the structure of the group attached to the nitrogen atom has been reported in our previous work where butyl and dodecyl chains have been used.[21] The appearance of the emission peak at 580 nm was attributed to aggregation of the complex in solution. This phenomenon was in fact the driving force behind the design of complexes **1** and **2** where the originally used alkyl chain was replaced by a more hydrophilic ethylene hydroxyl unit, expected to result in a more hydrophilic complex, which would be less likely to aggregate. This goal appears to have been achieved for complex **1**. Surprisingly Complex **2**, on the other hand appears to be even more prone to aggregation that the previously reported complex containing a

butyl chain as it exhibits the emission peak at 580 nm, which was absent in the case of the butyl chain containing complex.

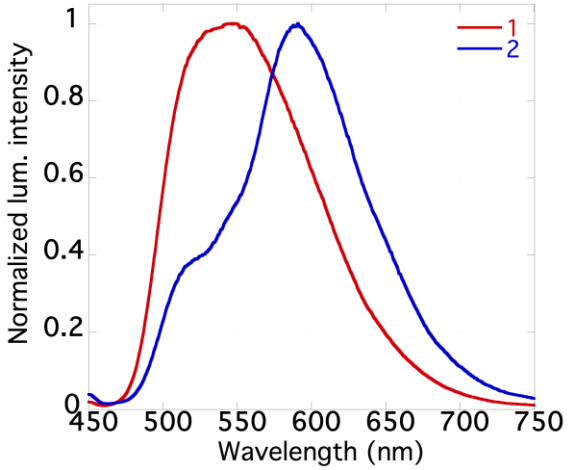

Figure 4. Normalized absorption and emission spectra of complexes **1** (red) and **2** (blue) (10 μM) recorded in water (λ_{ex} = 390 nm)

The decreased propensity of complex **1** to aggregate is demonstrated by its monoexponetial excited state decay in aqueous solution, where, on account of aggregation, the previously reported complexes, as well as complex **2** showed multiexponential decays (**SI Figure 8**). This is further demonstrated by the photophysical behavior in phosphate buffer solutions. In this case, at pH 7.5, the previously reported butyl complex (**Figure 1**) exhibited the presence of the emission peak at 580 nm assigned to aggregated form, as is also seen in the case of complex **2**. On the other hand, complex **1** still only contains a single emission peak at 530 nm (**SI Figure 9**).

The similarity of complex **2** to the parent butyl analogue and decreased propensity to aggregate for complex **1** is also shown in the plot of the ratio of emission intensity at 580 nm to emission intensity at 530 nm measured in phosphate buffer for the pH range 5.5 to 10.0 (**Figure 5**). It has been established, that for complex **1** this ratio at pH 5.5 has the value of 0.61 while for complex **2** the ratio value is 1.10. At pH 10.0, the emission intensity ratio values are 1.42 and 2.98 for complexes **1** and **2**, respectively. The corresponding intensity ratio values for the butyl complex were 0.83 and 5.03 at pH 5.5 and 10.0 respectively (**SI Figure 10**). This confirms, that the complexes are much more prone to aggregate at higher pH values as they exhibit higher values of the intensity ratio, which is understandable as at higher pH values the amino group become deprotonated making aggregation more favorable. Thus, at pH 10.0 even complex **2** exhibits decreased propensity to aggregate than the butyl complex, as was expected. We have previously discussed that both the hydrophilicity/hydrophobicity of the chains attached to the amino group and its protonation state affect the propensity to aggregate. The interplay of these factors is the likely explanation for the higher than expected propensity to aggregate for complex **2**. This is because diethanolamine, which it is based on, is the most hydrophilic of the three amines but also least basic (**SI Table 1**), meaning that at any given pH it contains the highest proportion of the molecules in the aggregation prone free base form.

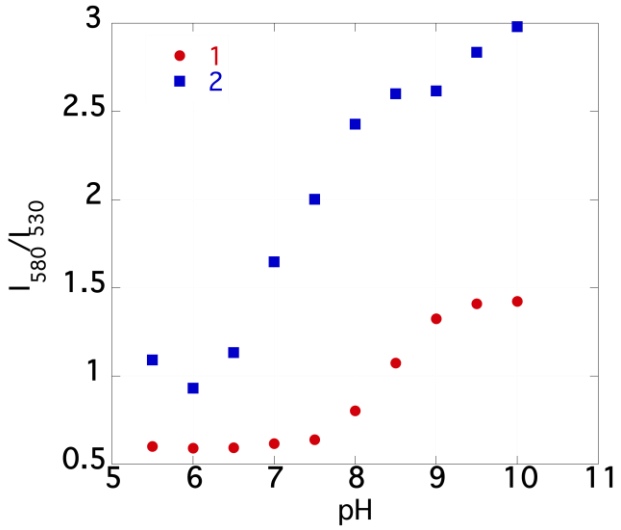

Figure 5. Plot of the ratio of emission intensity at 580 nm and 530 nm for complexes **1** and **2** versus pH

Cellular Experiments

Complexes **1** and **2** have been synthesized as part of our ongoing effort to investigate how the nature of aminoalkyl structure in these tris-cyclometalated iridium complexes affects their bio-compatibility and performance as potential stains for fluorescence microscopy. We have recently published a report on a quarternary ammonium salt of the butyl substituted complex, in addition to the previously mentioned report on the complexes bearing the butyl and dodecyl chain.[21-22] Our previously reported complexes have displayed lysosomal localization. However, the quarternary ammonium complex stood out in terms of its significantly lower cytotoxicity. **Figure 6** shows the plot of viability of NIH-3T3 cells incubated with complexes **1** and **2** for 24h. It can be seen, that complex **1** shows IC_{50} below 5 μM, which is similar to what was observed for the alkyl complexes. On the other hand, complex **2** shows significantly lower cytotoxicity with IC_{50} value on the order of 50 μM. Complex **2** is, in this respect, more similar to the quarternary ammonium complex, which has also shown lower cytoxicity than the simple aminoalkyl complexes.

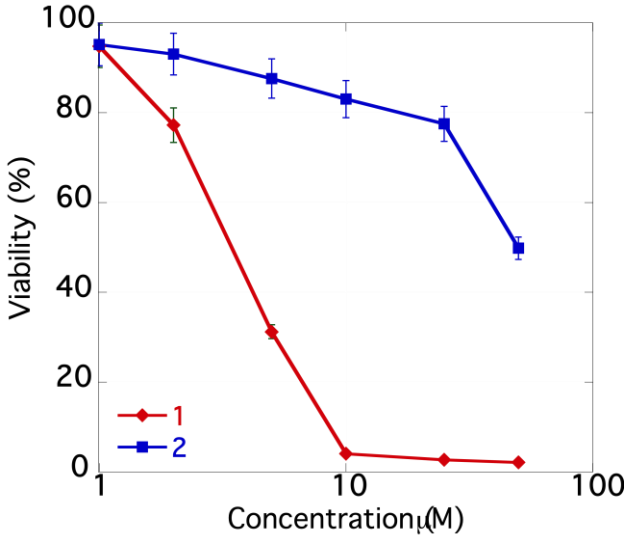

Figure 6. Plot of cellular viability of NIH-3T3 cells versus concentration for **1** and **2** (24 h)

ICP-MS analyses, which were carried out on cell lysates after incubation with complexes **1** and **2** do indicate that complex **1** exhibits higher intracellular concentration than complex **2**, which could, in part, provide explanation for the decreased cytotoxicity of complex **2**.

Figure 7 and **Figure 8** show the results of fluorescence (LSCM) imaging experiments with complexes **1** and **2**, respectively, in NIH-3T3 cells. The cellular localization of the two complexes is compared to that of lysotracter red. Images for complex **1** were acquired after 1 h incubation with 2 μM solution of the complex. The lower cytotoxicity of complex **2** allowed incubation with a 5 μM solution of the complex for two 2h, which resulted in better quality images. It can be seen, that complex **2** (**Figure 8**) exhibits lysosomal localization, analogous to that observed for our previously reported complexes. On the other hand, while there is some degree of overlap between the images obtained with complex **1** (**Figure 7**) and lysotracker red, complex **1** does show a more diffuse emission throughout the cytosol.

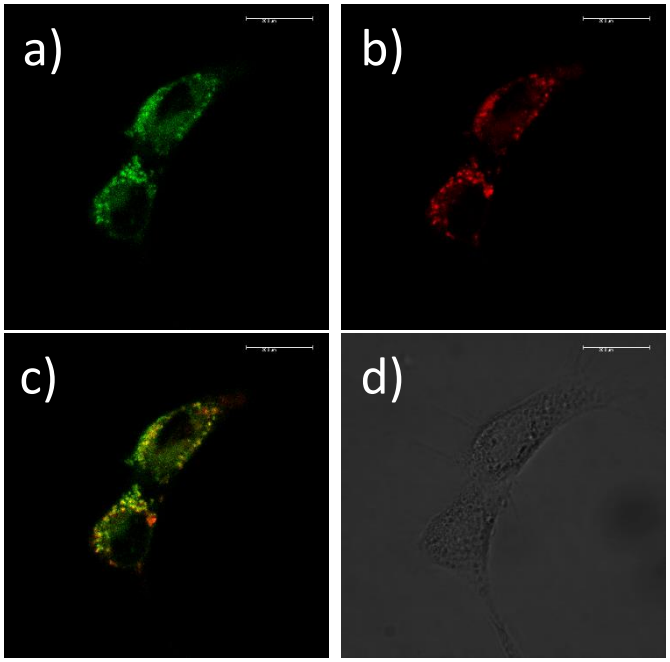

Figure 7. LSCM microscopy images of NIH-3T3 cells obtained with complex **1** (λ_{ex} 355 nm, λ_{em} 450-650 nm) (a), lysotacker red (λ_{ex} 543 nm HeNe laser, λ_{em} 600-650 nm) (b). Panel c shows the RGB overlay of panels and a b; P = 0.68, while panel d is the birghtfield image. (Scale bar: 20 μm)

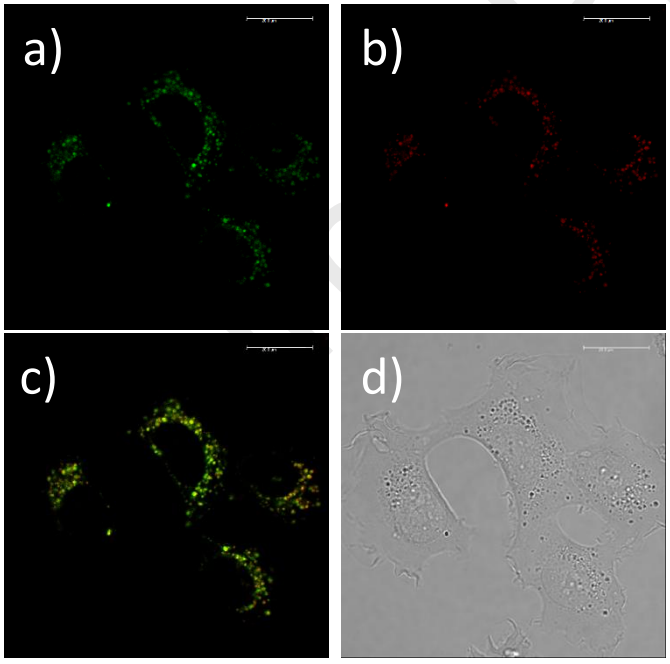

Figure 8. LSCM microscopy images of NIH-3T3 cells obtained with complex **1** (λ_{ex} 355 nm, λ_{em} 450-650 nm) (a), lysotacker red (λ_{ex} 543 nm HeNe laser, λ_{em} 600-650 nm) (b). Panel c shows the RGB overlay of panels and a b; P = 0.74, while panel d is the birghtfield image. (Scale bar: 20 μm)

Conclusions

In conclusion, two novel tris-cyclometalated iridum complexes have been synthesized and investigated. These complexes are analogues of our previously reported aminoalkyl complexes containing one (**1**) and two (**2**) hydroxylethyl groups on the nitrogen atoms. The photophysical properties of complexes **1** and **2** in organic solvent are similar to the parent complex *fac*-[Ir(ppy)$_3$] and our previously reported aminoalkyl complexes. In aqueous media, complex **1** exhibits the properties expected from the inclusion of the hydrophilic group on the nitrogen atom as evidenced by its decreased tendency to aggregate. Complex **2** shows properties that are intermediate between those of complex **1** and the previously reported complex containing a butyl chain, which is likely due to a lower basicity. Cellular imaging was achieved with both complexes, however, complex **2** is more promising in this respect given its lower cytotoxicity and better defined cellular localization.

Acknowledgements

This research was supported a grant from the Thailand Research Fund No. RSA6080041. The authors also acknowledge the National e-Science Infrastructure Consortium. S.M. also acknowledges scholarship support from the Science Achievement Scholarship of Thailand (SAST). RP acknowledges support form the Royal Society.

References

1. You, Y., Phosphorescence bioimaging using cyclometalated Ir(III) complexes. *Current opinion in chemical biology* **2013,** *17* (4), 699-707.
2. Caporale, C.; Massi, M., Cyclometalated iridium(III) complexes for life science. *Coordin Chem Rev* **2018,** *363*, 71-91.
3. You, Y.; Nam, W., Photofunctional triplet excited states of cyclometalated Ir(III) complexes: beyond electroluminescence. *Chemical Society reviews* **2012,** *41* (21), 7061-84.
4. König, B., Photocatalysis in Organic Synthesis - Past, Present, and Future. *European Journal of Organic Chemistry* **2017,** *2017* (15), 1979-1981.
5. Shaw, M. H.; Twilton, J.; MacMillan, D. W. C., Photoredox Catalysis in Organic Chemistry. *The Journal of organic chemistry* **2016,** *81* (16), 6898-6926.
6. Hu, Y.-X.; Xia, X.; He, W.-Z.; Tang, Z.-J.; Lv, Y.-L.; Li, X.; Zhang, D.-Y., Recent developments in benzothiazole-based iridium(Ⅲ) complexes for application in OLEDs as electrophosphorescent emitters. *Organic Electronics* **2019,** *66*, 126-135.
7. Li, T.-Y.; Wu, J.; Wu, Z.-G.; Zheng, Y.-X.; Zuo, J.-L.; Pan, Y., Rational design of phosphorescent iridium(III) complexes for emission color tunability and their applications in OLEDs. *Coordin Chem Rev* **2018,** *374*, 55-92.
8. Abbas, S.; Din, I. u. D.; Raheel, A.; Tameez ud Din, A., Cyclometalated Iridium (III) complexes: Recent advances in phosphorescence bioimaging and sensing applications. *Applied Organometallic Chemistry* **2019**.
9. Deng, Y.; Pan, S.; Zheng, J.; Hong, Y.; Liu, J.; Chang, H.; Miao, Y.; Sun, Y.; Li, Y., Electrostatic self-assembled Iridium(III) nano-photosensitizer for selectively disintegrated and mitochondria targeted photodynamic therapy. *Dyes and Pigments* **2020,** *175*.

10. Chirdon, D. N.; Transue, W. J.; Kagalwala, H. N.; Kaur, A.; Maurer, A. B.; Pintauer, T.; Bernhard, S., [Ir(N^N^N)(C^N)L]+: a new family of luminophores combining tunability and enhanced photostability. *Inorganic chemistry* **2014,** *53* (3), 1487-99.
11. Ladouceur, S.; Zysman-Colman, E., A Comprehensive Survey of Cationic Iridium(III) Complexes Bearing Nontraditional Ligand Chelation Motifs. *Eur J Inorg Chem* **2013,** *2013* (17), 2985-3007.
12. Zanoni, K. P.; Coppo, R. L.; Amaral, R. C.; Murakami Iha, N. Y., Ir(III) complexes designed for light-emitting devices: beyond the luminescence color array. *Dalton Trans* **2015,** *44* (33), 14559-73.
13. Thorp-Greenwood, F. L.; Balasingham, R. G.; Coogan, M. P., Organometallic complexes of transition metals in luminescent cell imaging applications. *J Organomet Chem* **2012,** *714*.
14. You, Y.; Seo, J.; Kim, S. H.; Kim, K. S.; Ahn, T. K.; Kim, D.; Park, S. Y., Highly phosphorescent iridium complexes with chromophoric 2-(2-hydroxyphenyl)oxazole-based ancillary ligands: interligand energy-harvesting phosphorescence. *Inorganic chemistry* **2008,** *47* (5), 1476-87.
15. Li, C.-J.; Yin, S.-Y.; Wang, H.-P.; Wei, Z.-W.; Pan, M., Tuning colorful luminescence of iridium(III) complexes from blue to near infrared. *Journal of Photochemistry and Photobiology A: Chemistry* **2019,** *379*, 99-104.
16. Coogan, M. P.; Fernandez-Moreira, V., Progress with, and prospects for, metal complexes in cell imaging. *Chem Commun (Camb)* **2014,** *50* (4), 384-99.
17. Fernandez-Moreira, V.; Thorp-Greenwood, F. L.; Coogan, M. P., Application of d6 transition metal complexes in fluorescence cell imaging. *Chem Commun (Camb)* **2010,** *46* (2), 186-202.
18. Hisamatsu, Y.; Aoki, S., Design and Synthesis of Blue-Emitting Cyclometalated Iridium(III) Complexes Based on Regioselective Functionalization. *Eur J Inorg Chem* **2011,** *2011* (35), 5360-5369.
19. Hisamatsu, Y.; Shibuya, A.; Suzuki, N.; Suzuki, T.; Abe, R.; Aoki, S., Design and Synthesis of Amphiphilic and Luminescent Tris-Cyclometalated Iridium(III) Complexes Containing Cationic Peptides as Inducers and Detectors of Cell Death via a Calcium-Dependent Pathway. *Bioconjug Chem* **2015,** *26* (5), 857-79.
20. Aoki, S.; Matsuo, Y.; Ogura, S.; Ohwada, H.; Hisamatsu, Y.; Moromizato, S.; Shiro, M.; Kitamura, M., Regioselective aromatic substitution reactions of cyclometalated Ir(III) complexes: synthesis and photochemical properties of substituted Ir(III) complexes that exhibit blue, green, and red color luminescence emission. *Inorganic chemistry* **2011,** *50* (3), 806-18.
21. Sansee, A.; Meksawangwong, S.; Chainok, K.; Franz, K. J.; Gal, M.; Palsson, L. O.; Puniyan, W.; Traiphol, R.; Pal, R.; Kielar, F., Novel aminoalkyl tris-cyclometalated iridium complexes as cellular stains. *Dalton Trans* **2016,** *45* (43), 17420-17430.
22. Meksawangwong, S.; Gohil, B.; Punyain, W.; Pal, R.; Kielar, F., Synthesis and investigation of a tris-cyclometalated iridium complex bearing a single quarternary ammonium group. *Inorganica chimica acta* **2019,** *497*.
23. Abe, T.; Miyazawa, A.; Konno, H.; Kawanishi, Y., Deuteration isotope effect on nonradiative transition of fac-tris (2-phenylpyridinato) iridium (III) complexes. *Chemical Physics Letters* **2010,** *491* (4-6), 199-202.
24. M. J. Frisch, G. W. T., H. B. Schlegel, G. E. Scuseria, M. A. Robb, J. R. Cheeseman, G. Scalmani, V. Barone, B. Mennucci, G. A. Petersson, H. Nakatsuji, M. Caricato, X. Li, H. P. Hratchian,

A. F. Izmaylov, J. Bloino, G. Zheng, J. L. Sonnenberg, M. Hada, M. Ehara, K. Toyota, R. Fukuda, J. Hasegawa, M. Ishida, T. Nakajima, Y. Honda, O. Kitao, H. Nakai, T. Vreven, J. A. Montgomery, Jr., J. E. Peralta, F. Ogliaro, M. Bearpark, J. J. Heyd, E. Brothers, K. N. Kudin, V. N. Staroverov, T. Keith, R. Kobayashi, J. Normand, K. Raghavachari, A. Rendell, J. C. Burant, S. S. Iyengar, J. Tomasi, M. Cossi, N. Rega, J. M. Millam, M. Klene, J. E. Knox, J. B. Cross, V. Bakken, C. Adamo, J. Jaramillo, R. Gomperts, R. E. Stratmann, O. Yazyev, A. J. Austin, R. Cammi, C. Pomelli, J. W. Ochterski, R. L. Martin, K. Morokuma, V. G. Zakrzewski, G. A. Voth, P. Salvador, J. J. Dannenberg, S. Dapprich, A. D. Daniels, O. Farkas, J. B. Foresman, J. V. Ortiz, J. Cioslowski, and D. J. Fox *Gaussian 09*, Gaussian, Inc.: Wallingford, CT, USA, 2009.

25. R., A. A., Gabedit - A Graphical User Interface for computational Chemistry Softwares. *Journal of Computational Chemistry* **2011,** *32*, 174-182.

26. Pal, R., Phase modulation nanoscopy: a simple approach to enhanced optical resolution. *Faraday Discuss* **2015,** *177*, 507-15.

Author Contributions:

Sureemas Meksawangwong: Invesitgation, Data Curation, Visualisation, Writing – Review and Editing

Bhavini Gohil: Investigation

Wikorn Punyain: Investigation, Visualization

Robert Pal: Investigation, Visualisation, Writing – Review and Editing, Funding acquisition

Filip Kielar: Conceptualization, Methodology, Writing – Original Draft, Writing Review and Editing, Supervision, Funding acquisition

Declaration of interests

☒ The authors declare that they have no known competing financial interests or personal relationships that could have appeared to influence the work reported in this paper.

☐The authors declare the following financial interests/personal relationships which may be considered as potential competing interests:

- Two novel tris-cyclometalated iridium complex containing aminoalkyl group with hydroxyethyl chains have been synthesized
- The photophysical properties of the iridium complexes in aqueous solution depend on the number of hydroxyl ethyl chains bound to the nitrogen atom
- The synthesized iridium complexes can be used as stains for fluorescence microscopy in live NIH-3T3 cells